NATIONAL ADVISORY COMMITTEE FOR AERONAUTICS

TECHNICAL NOTE

No. 1319

CALCULATIONS OF THE SUPERSONIC WAVE DRAG OF NONLIFTING WINGS WITH ARBITRARY SWEEPBACK AND ASPECT RATIO

WINGS SWEPT BEHIND THE MACH LINES

By Sidney M. Harmon and Margaret D. Swanson

Langley Memorial Aeronautical Laboratory
Langley Field, Va.

Washington
May 1947

NATIONAL ADVISORY COMMITTEE FOR AERONAUTICS

TECHNICAL NOTE NO. 1319

CALCULATIONS OF THE SUPERSONIC WAVE DRAG OF NONLIFTING WINGS WITH ARBITRARY SWEEPBACK AND ASPECT RATIO

WINGS SWEPT BEHIND THE MACH LINES

By Sidney M. Harmon and Margaret D. Swanson

SUMMARY

On the basis of a recently developed theory for finite swept-back wings at supersonic speeds, calculations of the supersonic wave drag at zero lift were made for a series of wings having thin symmetrical biconvex sections with untapered plan forms and various angles of sweepback and aspect ratios. The results are presented in a unified form so that a single chart permits the direct determination of the wave drag for this family of airfoils for an extensive range of aspect ratio and sweepback angle for stream Mach numbers up to a value corresponding to that at which the Mach line coincides with the wing leading edge.

The calculations showed that in general the wave-drag coefficient decreased with increasing sweepback. At Mach numbers for which the Mach lines are appreciably ahead of the wing leading edge, the wave-drag coefficient decreased to an important extent with increases in aspect ratio or slenderness ratio. At Mach numbers for which the Mach lines approach the wing leading edge (Mach numbers approaching a value equal to the secant of the angle of sweepback), the wave-drag coefficient decreased with reductions in aspect ratio or slenderness ratio.

INTRODUCTION

Recent developments in airfoil theory for supersonic speeds (references 1 and 2) indicate pronounced effects of sweepback and aspect ratio on the drag. In reference 1, a theory was developed for calculating the pressure distribution at supersonic speeds and zero lift for swept-back wings of arbitrary linear taper and aspect ratio having thin symmetrical airfoil sections of sharp leading edges.

In the present paper, the method of reference 1 is applied to calculate the supersonic wave drag for a series of wings having thin symmetrical biconvex sections at zero lift with untapered plan forms and various angles of sweepback and aspect ratios. The term "biconvex profile" as used herein refers to an airfoil section composed of two parabolic arcs. In each case, the wing is considered to be cut off in a direction parallel to the direction of flight. In the calculations the Mach number is varied from 1.0 to a value corresponding to that at which the Mach line coincides with the wing leading edge. The results of the calculations are presented in a unified form which permits the direct determination from a single chart of the wave drag for this family of wings for an extensive range of sweepback angle and aspect ratio for Mach numbers from 1.0 to the value corresponding to that at which the Mach line coincides with the wing leading edge, or equal to the secant of the angle of sweepback. Although the calculations have been made for the biconvex profile, the data may be applied to indicate corresponding results for profiles approximately similar to the biconvex.

SYMBOLS

x, y, z	coordinates of mutually perpendicular system of axis in wing
dz/dx	slope of airfoil surface
c	chord of airfoil section, measured in flight direction
t/c	thickness ratio of section, measured in flight direction
Λ	angle of sweep, degrees
$m = \cot \Lambda$	

h wing semispan measured along y-axis, semichords except in appendix A

K parameter indicating spanwise position equal to y/m, semichords

A aspect ratio

l/t slenderness ratio, ratio of wing semispan measured along leading edge to maximum thickness of center section

p disturbance pressure

p/q pressure coefficient, ratio of disturbance pressure to dynamic pressure in free stream

V velocity in flight direction

u x-component of disturbance velocity, positive in flight direction

$\bar{u}$ u caused by source line with reversal in sign of m

w z-component of disturbance velocity

ϕ disturbance-velocity potential

I source factor required to maintain a given wedge angle

M Mach number

$\beta = \sqrt{M^2 - 1}$

y_a coordinate measured along y-axis which is shifted to tip section, semichords

y_b coordinate measured along y-axis which is shifted to opposite tip section, semichords

d wave drag at section

c_{d_∞} wave-drag coefficient at section without tip effect

c_d wave-drag coefficient at section including tip effect

Δc_d increment in section wave-drag coefficient caused by wing tips

Δc_{d_I} increment in section wave-drag coefficient caused by wing tip located on same half of wing as section

$\Delta c_{d_{II}}$ increment in wave-drag coefficient at section on one wing panel caused by tip of opposite wing panel

C_{D_∞} wave-drag coefficient for wing without tip effect

C_D wave-drag coefficient for wing including tip effect

ΔC_D increment in wave-drag coefficient caused by tips, complete wing

ΔC_{D_I} increment in wave-drag coefficient on one wing panel caused by adjacent wing tip, complete wing

$\Delta C_{D_{II}}$ increment in wave-drag coefficient on one wing panel caused by tip of opposite wing panel, complete wing

ξ, η auxiliary variables which replace x and y, respectively, used to indicate origin of source line

Primed values of A, y, y_a, y_b, h, m, dz/dx, and z indicate transformation involving multiplication by factor β.

Subscripts:

1, 2 wings related according to transformation which makes $y\beta$ and $m\beta$ equal respectively for two wings

Subscript notations for u and $\bar{u}$ indicate the origin of source line in terms of coordinates x and y, respectively.

ANALYSIS

Basic data.- The present analysis is based on thin-airfoil theory for small pressure disturbances and a constant velocity of sound throughout the fluid. The axes used are the mutually perpendicular x, y, z system in which the x-axis is taken in the direction of flight positive to the rear, the y-axis is along the span positive to the right, and the z-axis is positive upwards. Figure 1 shows the symbols used to designate the wing-plan-form parameters. The present analysis is made for untapered wings of biconvex profile at zero lift and is limited to a Mach number range from 1.0 to the value corresponding to that at which the Mach line coincides with the wing leading edge, that is, to a value equal to the secant of the angle of sweepback.

Theory.- If p is the disturbance pressure computed for one surface of the airfoil section, the wave drag for the section is

$$d = 2\int_0^c p\,\frac{dz}{dx}\,dx \tag{1}$$

and the section wave-drag coefficient

$$c_d = \frac{2}{c}\int_0^c \frac{p}{q}\,\frac{dz}{dx}\,dx \tag{2}$$

where dz/dx is the slope of the surface of the airfoil at the point x. For the symmetrical biconvex profiles (composed of parabolic arcs)

$$\frac{dz}{dx} \approx \frac{4\frac{t}{c}}{c}\left(\frac{c}{2} - x\right)$$

where the thickness ratio t/c may be considered the sole shape parameter. From thin-airfoil theory,

$$\frac{p}{q} = -\frac{2}{V}\,\frac{\partial\phi}{\partial x} = 2\frac{u}{V}$$

where u is the disturbance-velocity component in the x-direction, taken positive in the flight direction. For a given swept-back wing with $\Lambda = \cot^{-1}m$, the drag coefficient in equation (2) at the spanwise station y may now be written as

$$c_d(y) = \frac{16\frac{t}{c}}{c^2}\int_{y/m}^{\frac{y}{m}+c} \frac{u}{V}\left(\frac{c}{2} - x + \frac{y}{m}\right) dx \tag{3}$$

The desired integrand u in equation (3) may be determined by the procedure given in reference 1. On the basis of the linearized theory, reference 1 derives a solution representing an oblique (swept-back) source line making the angle of sweepback Λ with the y-axis. This solution utilized for the pressure field or for the disturbance velocity is the real part of

$$u_{0,0} = I \cosh^{-1}\frac{x - m\beta^2 y}{\beta\left|y - mx\right|} \tag{4}$$

where the subscript notation indicates that the source line starts at the origin of coordinates $(x = 0,\ y = 0)$. Equation (4) is shown in reference 1 to satisfy the boundary condition for a thin oblique wedge making the half-angle $\left(\frac{dz}{dx}\right)'$ in the transformed coordinate system of reference 1 $(y' = y\beta,\ z' = z\beta)$ where $\left(\frac{dz}{dx}\right)' = \frac{w'}{V} = \frac{\pi}{V}\frac{\sqrt{1 - m'^2}}{m'}I$. In order to obtain an equal wedge angle in the physical coordinate system, the following relations between the transformed coordinates of reference 1 and the physical coordinates are used

$$m' = m\beta$$

$$w' = \frac{\partial\phi}{\partial z'}$$

$$w = \frac{\partial\phi}{\partial z}$$

where w' and w refer, respectively, to the vertical velocities in the transformed and physical coordinate systems. Thus

$$w = \frac{\partial \phi}{\partial z'} \frac{\partial z'}{\partial z} = w'\beta$$

The half-angle of the wedge is then determined as

$$\frac{dz}{dx} = \frac{w}{V} = \frac{\pi}{V} \frac{\sqrt{1 - m^2\beta^2}}{m} I$$

or the required source factor in order to maintain the desired wedge angle is

$$I = \frac{V}{\pi} \frac{m}{\sqrt{1 - m^2\beta^2}} \frac{dz}{dx} \tag{5}$$

By superposition of solutions of the wedge type, swept-back wings of desired profile shape and plan form can be built up (reference 1). In order to satisfy the boundary conditions over the surface of a biconvex wing, semi-infinite source lines of equal strength are placed along the leading and trailing edges beginning at the center section, in conjunction with a constant distribution of sink lines along the chord. At the tip, where the wing is cut off, reversed semi-infinite source and sink lines are distributed so as to cancel exactly the effect of those originating at the center section in the entire region of space outboard of the tip. In the present analysis, the tip is assumed to be cut off in the direction of flight. The term "tip effect" refers to the effect of this wing cut-off. The form of the integrand u for equation (3) is given in appendix A.

In calculating the wave drag over the wing, the disturbances due to the elementary sources and sinks are evidently limited to the regions enclosed by their Mach cones. Figure 2 shows the typical Mach lines originating from the source lines at the leading and trailing edges of the center and tip sections over a wing of

45° sweepback. Figure 2(a) shows the Mach lines for the infinitely long wing, and figure 2(b) includes the Mach lines starting from the tip section. In each case the disturbance over the wing caused by the leading- and trailing-edge source lines is limited to the region of the wing behind the corresponding Mach line. The regions affected by each of the Mach lines are indicated in figure 2(b) as regions I to IV. Region I represents the part of the wing affected by the sink line starting from the leading edge of the adjacent tip; region II represents the wing area affected by the sink line starting from the opposite tip. Region III is influenced by the source line starting at the leading edge of the center section and includes the entire wing; region IV is influenced by the source line starting at the trailing edge of the center section.

The resultant velocity u at a point on the wing is made of the component velocities caused by each of these source and sink lines where the influence of each component is restricted to the region behind its Mach line. The drag coefficient c_{d_∞} is therefore obtained by evaluating in equation (3) the integrand $u_{0,0}$ over the entire section (region III), the integrand $u_{c,0}$ over part of the section included in region IV, and the integrands for the u-components caused by the sink distributions along the profile (fig. 2(b) and appendix A, equation (A2)). The drag coefficients Δc_{d_I} and $\Delta c_{d_{II}}$ are obtained similarly by integrating along the section in the regions I and II, respectively, in addition to the integrations for the u-components caused by the source distributions along the profile (appendix A). The limits of integrations for x along the chord and for y along the span, which represent the boundaries for the regions of influence for the individual u-functions required for a biconvex profile, are given in the table in appendix A.

Formulas for section wave-drag coefficients.- The formulas for the section drag coefficients obtained by integration of the u-functions and by use of equation (3) are presented in appendix B. These formulas give expressions for the drag coefficient without the tip effect c_{d_∞} and also the expressions for the increments in c_d caused by the tip effect Δc_d.

Wave-drag coefficients for complete wing.- In the present investigation the section drag coefficients expressed by the equations in appendix B were integrated graphically to obtain the results for the wing-drag coefficients. Subsequently, however, analytical expressions for the integrations were obtained. These formulas for the wing-drag coefficients are presented in appendix B.

Drag coefficient of swept-back wing at Mach number of 1.0.- The solution of the equations for c_d given in appendix B shows that, for a symmetrical untapered finite swept-back wing at Mach number of 1.0 and zero lift, positive and negative infinite values for c_d are obtained at various sections of the wing. The integration over the wing of the limiting values for these infinite terms, however, gives zero. Although some sections of the wing have infinitely positive or negative drag, the total drag coefficient over the wing results in a finite value. The prediction of infinite values of drag at certain sections of the wing clearly violates at these sections the assumption of small disturbances from which the linearized theory is derived. The calculated values for the total drag coefficient at Mach number 1.0 are therefore questionable. The formulas for the total drag at Mach number 1.0 are presented in appendix B.

Conversion of drag solution to series of related wings.- An examination of equations (B1), (B3), and (B5) indicates that the drag solution obtained for one value of m and M may be applied directly to obtain the drag for a whole series of wings in which each wing is at a certain appropriate Mach number. (Equation (B1) is formed by adding expression (B1b) to the right-hand side of equation (B1a).) For example, equation (B1) may be expressed in the following form:

$$c_{d_\infty}(y) = \frac{8}{\pi}\left(\frac{t}{c}\right)^2 \frac{m\beta}{\beta} F\left(\frac{y\beta}{m\beta}, m\beta\right) \tag{6}$$

where $F\left(\frac{y\beta}{m\beta}, m\beta\right)$ refers to the variable terms and where $m\beta = m'$, and $\frac{y}{m} = K$. If the subscript 1 refers to a wing at Mach number corresponding to β_1 and the subscript 2 to any other wing at the Mach number corresponding to β_2, then the drag coefficients for the two wings may be obtained from equation (6) as follows:

$$c_{d_{\infty_1}} = \frac{8}{\pi}\left(\frac{t}{c}\right)_1^2 \frac{m_1\beta_1}{\beta_1} F\left(\frac{y_1\beta_1}{m_1\beta_1}, m_1\beta_1\right) \tag{7a}$$

$$c_{d_{\infty_2}} = \frac{8}{\pi}\left(\frac{t}{c}\right)_2^2 \frac{m_2\beta_2}{\beta_2} F\left(\frac{y_2\beta_2}{m_2\beta_2}, m_2\beta_2\right) \tag{7b}$$

Equation (7) shows that if $y_1\beta_1 = y_2\beta_2$ and $m_1\beta_1 = m_2\beta_2$

$$c_{d_{\infty_1}} = c_{d_{\infty_2}} \frac{(t/c)_1^{\,2}}{(t/c)_2^{\,2}} \frac{\beta_2}{\beta_1} = c_{d_{\infty_2}} \frac{(t/c)_1^{\,2} \cot \Lambda_1}{(t/c)_2^{\,2} \cot \Lambda_2} \tag{8}$$

where $c_{d_{\infty_1}}$ and $c_{d_{\infty_2}}$ refer to the spanwise positions y_1 and $\frac{y_1\beta_1}{\beta_2}$, respectively. In a similar manner, it can be shown that if two wings are related according to $y_1\beta_1 = y_2\beta_2$ and $m_1\beta_1 = m_2\beta_2$, the section drag coefficients obtained for wings 1 and 2 from equations (B3) and (B5) are in the same ratio as that expressed in equation (8). Equation (8), therefore, may be generalized to apply to the total drag coefficient at the section or,

$$c_{d_1} = c_{d_2} \frac{(t/c)_1^{\,2} \cot \Lambda_1}{(t/c)_2^{\,2} \cot \Lambda_2} \tag{9}$$

where c_{d_1} and c_{d_2} refer to the spanwise positions y_1 and $\frac{y_1\beta_1}{\beta_2}$, respectively.

The wing-drag coefficients for wings 1 and 2 are given, respectively, by

$$C_{D_1} = \frac{1}{h_1}\int_0^{h_1} c_{d_1}\, dy_1 \tag{10}$$

$$C_{D_2} = \frac{1}{h_2}\int_0^{h_2} c_{d_2}\, dy_2 \tag{11}$$

By substituting for the integrand c_{d_1} in equation (10) the relationship expressed in equation (9) and by substituting $\frac{dy_2\beta_2}{\beta_1}$ for dy_1, equation (10) may be written as:

$$C_{D_1} = \frac{(t/c)_1^{\,2} \cot \Lambda_1}{h_2(t/c)_2^{\,2} \cot \Lambda_2}\int_0^{h_2} c_{d_2}\, dy_2$$

or

$$C_{D_1} = C_{D_2}\frac{(t/c)_1^{\,2} \cot \Lambda_1}{(t/c)_2^{\,2} \cot \Lambda_2} \tag{12}$$

Equation (12) permits a rapid determination of the drag coefficient for wings of arbitrary sweepback, aspect ratio, and thickness ratio (within limitations of airfoil theory) from data obtained for one swept-back wing for the appropriate range of aspect ratio and Mach number. For this purpose, use of a wing of 45° sweepback as the reference wing is most convenient. If the subscript 2 is used to refer to the parameters for the wing of 45° sweepback and the subscript 1 is dropped, equation (12) becomes

$$C_D = \frac{C_{D_2}\,(t/c)^2 \cot \Lambda}{(t/c)_2^{\,2}} \tag{13}$$

where C_D and C_{D_2} refer to wings whose aspect ratios and Mach numbers are related by the following equations:

$$A_2 = A \tan \Lambda \tag{14}$$

$$\beta_2 = \beta \cot \Lambda \tag{15}$$

The foregoing analysis shows that the results obtained for a wing of 45° sweepback and a given aspect ratio A_2 can be transformed by means of equation (13) to all wings for which the aspect-ratio parameter $A \tan \Lambda = A_2$ and the Mach number parameter $\beta \cot \Lambda = \beta_2$.

The grouping of the parameters as indicated in the foregoing analysis permits the use of a single generalized chart for presenting the drag results. This chart is discussed in the section entitled "Results and Discussion."

Prandtl-Glauert rule modified for supersonic flows.- In considering the linearized problem of supersonic flow past a wing, it is often convenient to refer the supersonic results for a given wing to a transformed wing at a reference Mach number of $M^2 = 2$. If this transformation is used a rule resembling the Prandtl-Glauert rule (reference 3) for the subsonic case, where $M = 0$ is the reference Mach number, may be obtained. This rule may be stated as follows:

The streamline field of the supersonic flow for a given body at a stream Mach number M may be calculated by multiplying the given y- and z-dimensions, including those for the Mach lines, by the factor $\sqrt{M^2 - 1}$ and then by calculating the flow about the resulting transformed body at the Mach number $\sqrt{2}$. The pressure p and velocity increments u for the given body at the Mach number M can then be obtained by multiplying the calculated pressure p and velocity increments u at corresponding points of the transformed body by the factor $\frac{1}{M^2 - 1}$.

It is interesting to note that the derivation of formulas (13) to (15) as given in this paper corresponds to utilizing the solution for a transformed wing for the whole family of wings related to this transformation and then applying the aforementioned modified Prandtl-Glauert rule.

RESULTS AND DISCUSSION

Variation of section drag coefficient along span.- Figure 2, which was introduced previously to illustrate the system of Mach lines, also shows the variation of section drag coefficient c_d along the span. The data are presented for a wing of 45° sweepback and thickness ratio of 0.10. Figure 2(a) gives the results for a wing of infinite aspect ratio and figure 2(b) gives the results for a wing of finite span.

In figure 2(a), the data are shown for Mach numbers of 1.100, 1.343, and 1.414. The lowest Mach number 1.100 represents a case in which the wing leading edge diverges rapidly from the Mach line (upper part of fig. 2(a)). In this case, the section drag coefficient c_d has a maximum value of 0.0542 at the center section, then drops sharply to zero at a distance of 1.13 chords from the center line. Beyond this point, the wing shows a negative drag, which approaches asymptotically the subsonic value of zero at an infinite distance from the wing center. This type of wave-drag distribution is similar to that indicated in figure 11 of reference 1 for a wing of 60° sweepback at a Mach number of 1.4.

For the higher Mach number 1.343, the spanwise variation of c_d is markedly flatter. Unlike the preceding case, the drag coefficient does not have its maximum value at the center section but, at first, increases in the outboard direction, then reaches a peak and falls to zero at a distance from the center of 6.6 chords (not shown in fig. 2(a)).

At the highest Mach number 1.414, the Mach line becomes coincident with the wing leading edge. In this case, the wing gives a very high drag and the section drag coefficient increases in the outboard direction, approaching infinity at an infinite distance from the wing center.

Figure 2(b) illustrates the condition at which the aspect ratio is less than $1/\sqrt{M^2 - 1}$. The calculated case shown is for an aspect ratio of 1.86 and Mach number of 1.10. In this case, the two wing tips cause increments in section drag coefficient on each half of the wing, namely, Δc_{d_I} and $\Delta c_{d_{II}}$. The tip effect Δc_{d_I} at a given distance from the tip is independent of the aspect ratio. The tip effect $\Delta c_{d_{II}}$, however, is a function of the aspect ratio.

Effect of wing tip on wing-drag coefficient.- Figure 3 shows the typical variation with aspect ratio of the increment in C_D due to the tip ΔC_D. The data are shown for a wing of 45° sweepback and a thickness ratio of 0.10 for Mach numbers of 1.100, 1.343, and 1.414. The present analysis for the untapered wings indicated that if the aspect ratio is equal to or greater than $2m/(m\beta + 1)$, the integrated value of Δc_{d_I} over the wing is zero. On this basis, if the aspect ratio of the wing is greater than $1/\sqrt{M^2 - 1}$, the total increment in drag contributed by tip is zero. As the aspect ratio is reduced, the tip effect $\Delta C_{D_{II}}$ which occurs when the aspect ratio is smaller than $1/\sqrt{M^2 - 1}$, however, leads to an increase in C_D. The tip effect ΔC_D then reaches a peak value at a certain aspect ratio, but as this aspect ratio is further decreased, ΔC_D drops sharply. In this case, at aspect ratios of approximately 0.5, ΔC_D becomes zero and assumes large negative values with further reductions in aspect ratio. For applications to very small aspect ratios, however, the theory may require modifications. The data in figure 3 show that as the Mach number is increased, the aspect ratio corresponding to zero value of ΔC_D becomes smaller.

The tip effects shown in figure 3 for the wing of 45° sweepback are similar for other wings of different sweepback at appropriate aspect ratios. The conversion formulas indicated in the section entitled "Analysis" indicate that the aspect-ratio effects for wings of different sweepback correspond qualitatively for equal values of the aspect-ratio parameter $A \tan \Lambda$. The Mach numbers for each of the wings differ, however. An aspect ratio of 0.8 (fig. 3) for the wing of 45° sweepback at a Mach number of 1.10 for example corresponds to an aspect ratio of $0.8 \cot \Lambda$ at a Mach number equal to $\sqrt{1 + \left[(1.10)^2 - 1\right] \tan^2 \Lambda}$ for any other wing of sweepback angle Λ.

Variation of wing-drag coefficient with Mach number, sweepback, and slenderness ratio.- Figure 4 shows the variation of C_D with M' for different sweepback angles with constant slenderness ratios. The slenderness ratio represents the ratio of the wing semispan measured along the leading edge to the maximum thickness of the center section. The data are presented for sweepback angles of 30°, 45°, 52.5°, and 60° with slenderness ratios of 25 and 50. The wings in figure 4 for the different slenderness ratios and sweepback angles are assumed to have the same wing area and the same profile normal to the wing leading edge. The slenderness ratios are based on a thickness ratio of 0.10 measured in a direction normal to the wing leading edge. The thickness ratio t/c measured in the flight direction, therefore, varies with sweepback as $\cos \Lambda$ or is equal to $0.1 \cos \Lambda$. The aspect ratio is reduced with sweepback by the factor $\cos^2\Lambda$. The aspect ratio is related to the slenderness ratio by the formula:

$$A = 0.2 \left(\frac{l}{t}\right) \cos^2\Lambda$$

The plan forms for the different wings are shown in figure 4.

The results in figure 4 show that, in general, the drag coefficient decreases with increasing sweepback. At Mach numbers for which the Mach lines are appreciably ahead of the wing leading edge, increasing the slenderness ratio or aspect ratio gives important reductions in calculated wave-drag coefficient. At Mach numbers for which the Mach lines approach the wing leading edge $(M \longrightarrow \sec \Lambda)$, however, short wide wings give appreciable reductions in wave-drag coefficient. The figure also indicates that the highest wave-drag coefficients for the normal range of aspect ratio occur at a Mach number equal to $\sec \Lambda$.

Effect of aspect ratio on wing-drag coefficient.- Figure 5 indicates the effect of aspect ratio on the wave-drag coefficient for the wing. The data in figure 5 show the wave-drag-coefficient parameter $\frac{C_D \tan \Lambda}{100\ (t/c)^2}$ plotted against the aspect-ratio parameter $A \tan \Lambda$. These results are shown for various values of the Mach number parameter $\sqrt{M^2 - 1} \cot \Lambda$, which correspond to a range of Mach number from 1.0 to the secant of the angle of sweepback, or $1 \leqq M \leqq \sec \Lambda$.

Figure 5 shows that for a given value of the Mach number parameter, the maximum wave-drag coefficient occurs at a definite aspect ratio. For example, if $\Lambda = 45^\circ$ and $\sqrt{M^2 - 1} \cot \Lambda = 0.310$ that is, $M = 1.05$) the maximum value of C_D occurs at an aspect ratio of 0.85. If the aspect ratio is decreased to values smaller than 0.85, C_D drops very sharply. Similarly, as the aspect ratio is increased from 0.85, C_D also decreases. Thus, in general for the Mach number parameter corresponding to $\sqrt{M^2 - 1} \cot \Lambda = 0.310$ the maximum value of C_D occurs at an aspect ratio equal to $0.85 \cot \Lambda$.

Application of curves of figure 5 to wings of arbitrary sweepback and aspect ratio.- The scale labels and curves of figure 5 apply to the series of wings that may be derived from a basic 10-percent-thick, 45° swept-back wing. The labels express the transformation equations (13) to (15). If Λ is set equal to 45° and t/c is set equal to 0.10 in these labels to correspond to the basic wing, the ordinates become simply C_D, the abscissa A (aspect ratio), and the curve parameter $\sqrt{M^2 - 1}$. The results in figure 5 may be applied to all swept-back wings covering a range of aspect ratio from 0 to 10 cot Λ corresponding to a range of Mach number from 1.0 to sec Λ. The data apply specifically to untapered wings with biconvex profiles at zero lift with the wing tips cut off in the direction of flight. The results, however, may be applied to indicate approximate results for profiles similar to the biconvex.

The following example is given in order to illustrate the use of figure 5. For a given wing

$$\Lambda = 70^\circ$$

$$A = 3$$

$$\frac{t}{c} = 0.08$$

$$M = 2.20$$

In order to find C_D:

$$A \tan \Lambda = 8.24$$

$$\sqrt{M^2 - 1} \cot \Lambda = 0.715$$

From figure 5, for $A \tan \Lambda = 8.24$ and $\sqrt{M^2 - 1} \cot \Lambda = 0.715$

$$\frac{C_D \tan \Lambda}{100 \, (t/c)^2} = 0.0123$$

therefore

$$C_D = 0.00286$$

CONCLUDING REMARKS

A theoretical investigation has been made of the supersonic wave drag of untapered swept-back wings at zero lift. The wing sections were biconvex and the wing tips were considered to be cut off in the direction of flight. The investigation was limited to a range of stream Mach number from 1.0 to a value corresponding to that at which the Mach line coincided with the wing leading edge. For this range of Mach number, the following conclusions have been drawn:

1. In general, the calculated wave-drag coefficient decreased with increasing sweepback.

2. At Mach numbers for which the Mach lines are appreciably ahead of the wing leading edge, increasing the slenderness ratio or aspect ratio gave important reduction in the calculated wave-drag coefficient.

3. At Mach numbers for which the Mach lines approach the wing leading edge (Mach numbers approaching a value equal to the secant of the angle of sweepback), decreasing the slenderness ratio or aspect ratio reduced the calculated wave-drag coefficient.

4. The highest calculated wave-drag coefficients for the normal range of aspect ratio occurred at a Mach number equal to the secant of the angle of sweepback.

5. The maximum wave-drag coefficient occurred at a definite aspect ratio which is determined by the Mach number and angle of sweepback.

6. For aspect ratios greater than $1/\sqrt{M^2 - 1}$, where M is the Mach number, the increment in wave-drag coefficient for the wing contributed by the tip was zero.

7. The variation of the drag with Mach number obtained for one sweepback angle for appropriate aspect ratios may be presented

in a unified form so that the drag for the complete range of sweepback angle, aspect ratio, and Mach number may be directly determined from a single chart.

Langley Memorial Aeronautical Laboratory
National Advisory Committee for Aeronautics
Langley Field, Va., December 17, 1946

APPENDIX A

FORMULAS FOR THE INTEGRAND u IN EQUATION (3) FOR FINITE UNTAPERED SWEPT-BACK WINGS OF BICONVEX PROFILE AT ZERO LIFT $\left[m = \cot\Lambda \leqq \frac{1}{\beta}\right]$

In order to satisfy the boundary condition for a finite swept-back wing of biconvex profile, the integrand u in equation (3) may be expressed in terms of components caused by elementary source lines as follows:

$$
\begin{aligned}
u = {} & u_{0,0} + u_{c,0} + \bar{u}_{0,0} + \bar{u}_{c,0} \\
& - \left(\frac{1}{D}u_{0,0} - \frac{1}{D}u_{c,0} + \frac{1}{D}\bar{u}_{0,0} - \frac{1}{D}\bar{u}_{c,0}\right) \\
& - \left[u_{h/m,h} + \bar{u}_{h/m,-h} - \left(\frac{1}{D}u_{h/m,h} + \frac{1}{D}\bar{u}_{h/m,-h}\right)\right] \qquad \text{(A1)}
\end{aligned}
$$

where the subscript notation indicates the origin of the source line. The bars over u refer to the source lines caused by the opposite wing panel; that is, $\bar{u}$ indicates a source line with a reversal in the sign of m.

In equation (A1), the u-functions are given by the real parts of the following expressions:

$$u_{\xi,\eta}(x,\ y) = I \cosh^{-1} \frac{x - \xi - m\beta^2(y - \eta)}{\beta\left|y - \eta - m(x - \xi)\right|}$$

$$\bar{u}_{\xi,\eta}(x,\ y) = I \cosh^{-1} \frac{x - \xi + m\beta^2(y - \eta)}{\beta\left|y - \eta + m(x - \xi)\right|}$$

where ξ, η represents the origin of the elementary source lines. For the biconvex profile,

$$\frac{dz}{dx} = 2\frac{t}{c}$$

and from equation (5), the factor

$$I = 2\frac{t}{c}\frac{V}{\pi}\frac{m}{\sqrt{1 - m^2\beta^2}}$$

The symbol $\frac{1}{D}$ in equation (A1) refers to an integration operation which represents the influence of a uniform distribution of source lines along the chord of the biconvex profile beginning at the position ξ, η. This symbol is defined by the following expressions:

$$\frac{1}{D}u_{\xi,\eta}(x, y) = \int_{x-\beta|y-\eta|}^{\xi} \frac{dI}{d\xi'} \cosh^{-1} \frac{x - \xi' - m\beta^2(y - \eta)}{\beta|y - \eta - m(x - \xi')|} d\xi'$$

$$= (y - \eta)\frac{dI}{dx}\left\{\frac{\sqrt{1 - m^2\beta^2}}{m} \cosh^{-1} \frac{x - \xi}{\beta|y - \eta|}\right.$$

$$\left. - \frac{1}{m}\left[1 - \frac{m(x - \xi)}{y - \eta}\right] \cosh^{-1} \frac{\left|\frac{x - \xi}{\beta(y - \eta)} - m\beta\right|}{\left|1 - \frac{m(x - \xi)}{y - \eta}\right|}\right\} \tag{A2}$$

where ξ' is the variable of integration representing the ξ-coordinate of the origin of each source line in the distribution of source lines.

For a biconvex profile

$$\frac{dI}{dx} = -\frac{V}{\pi}\frac{m}{\sqrt{1 - m^2\beta^2}}\frac{d^2z}{dx^2}$$

$$= \frac{4}{c}(t/c)\frac{V}{\pi}\frac{m}{\sqrt{1 - m^2\beta^2}}$$

Equation (A2) may be expressed as a function of $\frac{x - \xi}{y - \eta}$; that is,

$$\frac{1}{D}u_{\xi,\eta}(x, y) = (y - \eta)\, f\left(\frac{x - \xi}{y - \eta}\right)$$

Then

$$\frac{1}{D}u_{\xi,\eta}(x, y) = -(y - \eta)\, f\left[\frac{x - \xi}{-(y - \eta)}\right]$$

The limits of integrations with regard to x for the section drag coefficients and with regard to y for the total wing-drag coefficients are discussed. The u-components caused by each of the elementary source lines are zero at all points outside of the respective Mach cones. The functions for the u-integrand in equation (3) are therefore evaluated along the section for values of x beginning at the forward boundary of the Mach cone. This integration gives the section-drag-coefficient components. Similarly, in order to obtain the wing-drag coefficient, the section drag coefficient components obtained from the respective u-functions are evaluated along the wing span for values of y contained within the Mach cone. The following table refers to one side of the wing (x and y positive) and shows the limits of integration for x and y for the required u-functions:

u-components	Limits of integration			
	x		y	
	Lower limit	Upper limit	Lower limit	Upper limit
$u_{0,0}$ $\bar{u}_{0,0}$ $\frac{1}{D}u_{0,0}$ $\frac{1}{D}\bar{u}_{0,0}$	y/m	$\frac{y}{m} + c$	0	h
$u_{c,0}$ $\bar{u}_{c,0}$ $\frac{1}{D}u_{c,0}$ $\frac{1}{D}\bar{u}_{c,0}$	$y\beta + c$	$\frac{y}{m} + c$	0	h
$u_{h/m,h}$ $\frac{1}{D}u_{h/m,h}$	$\frac{h}{m}(m\beta + 1) - y\beta$	$\frac{y}{m} + c$	$h - \frac{mc}{m\beta + 1}$ $\left(\text{if} \quad A > \frac{2m}{m\beta + 1}\right)$ $0 \quad \left(\text{if} \quad A \leq \frac{2m}{m\beta + 1}\right)$	h
$\bar{u}_{h/m,-h}$ $\frac{1}{D}\bar{u}_{h/m,-h}$	$y\beta + \frac{h}{m}(m\beta + 1)$	$\frac{y}{m} + c$	$\frac{h(m\beta + 1) - mc}{1 - m\beta}$ $\left(\text{if} \quad A > \frac{2m}{m\beta + 1}\right)$ $0 \quad \left(\text{if} \quad A \leq \frac{2m}{m\beta + 1}\right)$	h

APPENDIX B

FORMULAS FOR WAVE-DRAG COEFFICIENTS FOR FINITE UNTAPERED SWEPT-BACK WINGS OF SYMMETRICAL BICONVEX PROFILE AT ZERO LIFT $\left[m = \cot\Lambda \leqq \frac{1}{\beta}\right]$

Section Drag Coefficients

In the following analysis the quantities y and K are employed nondimensionally in terms of the semichord. The equations for the drag coefficients in all cases refer to the real parts of the indicated expressions.

Section drag coefficients without tip effect.- The section drag coefficient for the given wing at a spanwise position y and Mach number M without the tip effect was found to be as follows:

The term $\frac{2m}{1 - m\beta}$ represents a convenient integration limit which indicates the intersection of the Mach line from the center-section trailing edge with the wing leading edge. For $y = Km < \frac{2m}{1 - m\beta}$

$$c_{d_\infty}(y) = \frac{8}{\pi}\left(\frac{t}{c}\right)^2 m\left(K^3\left(\cosh^{-1}\frac{K+2}{Km'} - 2\cosh^{-1}\frac{1}{m'}\right)\right.$$
$$+ \frac{1}{3\sqrt{1 - m'^2}}\left\{2\cosh^{-1}\frac{K\left(1 - m'^2\right) + 2}{2m'}\right.$$
$$- 2\left(2K^3 - 3K - 1\right)\cosh^{-1}\frac{K\left(1 + m'^2\right) + 2}{2m'(K + 1)}$$
$$+ 4K\left(2K^2 - 3\right)\cosh^{-1}\frac{1 + m'^2}{2m'} + K^2\left[2K\left(1 - m'^2\right)\right.$$
$$\left.\left.\left. - \sqrt{\left(1 - m'^2\right)\left[(K + 2)^2 - (Km')^2\right]}\right]\right\}\right) \qquad \text{(B1a)}$$

For $y = Km > \frac{2m}{1 - m\beta}$, the following expression is added to equation (B1a).

$$\frac{8}{\pi}\left(\frac{t}{c}\right)^2 m \left\{K^3 \cosh^{-1}\frac{K-2}{Km'} - \frac{1}{3\sqrt{1-m'^2}}\left[2\cosh^{-1}\frac{K\left(1-m'^2\right)-2}{2m'} + 2\left(2K^3 - 3K + 1\right)\cosh^{-1}\frac{K\left(1+m'^2\right)-2}{2m'(K-1)} + K^2\sqrt{\left(1-m'^2\right)\left[(K-2)^2 - (Km')^2\right]}\right]\right\} \tag{B1b}$$

where $m' = m\beta$.

For the special case $m = \frac{1}{\sqrt{M^2 - 1}}$, the Mach line coincides with the wing leading edge, and the expression for the drag coefficient obtained as a limiting case $(m' \longrightarrow 1)$ for all values of y becomes:

$$c_{d_\infty}(y) = \frac{8}{\pi}\left(\frac{t}{c}\right)^2 m \left\{y'^3 \cosh^{-1}\frac{y'+2}{y'} - \frac{2}{3}\left[\frac{y'(3y'+4)(y'-1)-2}{\sqrt{y'+1}}\right]\right\} \tag{B2}$$

where

$$y' = y\beta$$

At the center section, where y or $K = 0$, equation (B1a) becomes:

$$c_{d_\infty} = \frac{32}{3\pi}\left(\frac{t}{c}\right)^2 \frac{m}{\sqrt{1 - m^2\beta^2}} \cosh^{-1}\frac{1}{m\beta}$$

At the center section, for $y = 0$ and $m = \frac{1}{\beta}$, equation (B2) becomes:

$$c_{d_\infty} = \frac{32}{3\pi}\left(\frac{t}{c}\right)^2 m$$

Increment in section drag coefficient caused by wing tips.- The increment in c_d caused by the tips depends on various factors, such as the sweep angle, aspect ratio, and Mach number. The following types occur in an untapered wing:

I. If the aspect ratio of the wing is equal to or greater than $1/\sqrt{M^2 - 1}$ each tip affects solely its own half of the wing. In this case the effect of the tip is limited to the region of the wing outboard and rearward of the front Mach line originating from this tip. (See fig. 2(b).) The region of the wing affected is between values of y from $h - \frac{2m}{m\beta + 1}$ to h.

The increment in section drag coefficient at a Mach number M and spanwise position y caused by the tip was found to be as follows:

$$\Delta c_{d_I}(y) = \frac{8}{\pi}\left(\frac{t}{c}\right)^2 m \left\{\frac{y_a'}{12m'^2}\left[\left(y_a'^2 \frac{2 + m'^2}{m'} - 12m'\right) \cosh^{-1}\frac{y_a' + 2m'}{|m'y_a'|} + \left(2m' - 3y_a'\right)\sqrt{\left(\frac{y_a'}{m'} + 2\right)^2 - y_a'^2}\right] - \frac{2}{3\sqrt{1 - m'^2}} \cosh^{-1}\frac{\left(1 - m'^2\right)y_a' + 2m'}{2m'^2}\right\} \quad \text{(B3)}$$

where the subscript a indicates that the x-axis is shifted to the tip section, and $y_a' = y_a\beta$ and $m' = m\beta$. In the plan form of the wing

$$y = h + y_a$$

In equation (B3) values for y_a may be taken from $-\frac{2m}{m\beta + 1}$ to 0. When the Mach line is coincident with the leading edge of the airfoil; that is, $m = \frac{1}{\sqrt{M^2 - 1}}$, the expression for Δc_{d_I} becomes:

$$\Delta c_{d_I}(y) = \frac{4}{\pi}\left(\frac{t}{c}\right)^2 m\left[\frac{y_a'\left(y_a'^2 - 4\right)}{2}\cosh^{-1}\frac{y_a' + 2}{\left|y_a'\right|} - \frac{\sqrt{y_a' + 1}}{3}\left(3y_a'^2 - 2y_a' + 4\right)\right] \tag{B4}$$

II. If the aspect ratio of the wing is less than $\frac{1}{\sqrt{M^2 - 1}}$, the tip on the opposite wing contributes an increment in c_d in addition to that discussed under type I. The increment in c_d at a section caused by the opposite tip was obtained in the following form:

$$\begin{aligned}
\Delta c_{d_{II}}(y) = \frac{8}{\pi}\left(\frac{t}{c}\right)^2 m\Bigg(\frac{y_b'}{m'^3}\Bigg\{&\frac{1}{12}\left(7y_b' - 10h' - 2m'\right)\sqrt{\left[y_b' - 2(h' - m')\right]^2 - \left(m'y_b'\right)^2} \\
&- \left[\frac{y_b'^2}{12}\left(14 + m'^2\right) - 3h'y_b' + 2h'^2 - m'^2\right]\left[\cosh^{-1}\frac{y_b' - 2(h' - m')}{m'y_b'}\right]\Bigg\} \\
&+ \frac{2}{3m^3\sqrt{1 - m'^2}}\left[2y_b'^3 - 6y_b'^2h' + 3y_b'\left(2h'^2 - m'^2\right) - 2h'^3 + 3m'^2h' - m'^3\right] \\
&\left[\cosh^{-1}\frac{y_b'\left(1 + m'^2\right) - 2(h' - m')}{2m'\left(y_b' - h' + m'\right)}\right]\Bigg)
\end{aligned} \tag{B5}$$

where the subscript b indicates that the x-axis is shifted to the opposite tip section, and where $y_b' = y_b\beta$, $m' = m\beta$, and $h' = h\beta$. In the plan form of the wing

$$y = y_b - h.$$

The limits for y_b to be used in equation (B5) depend on the value of aspect ratio A relative to the parameter $\frac{2m}{m\beta + 1}$. Thus

(a) If the aspect ratio of the wing is greater than $\frac{2m}{m\beta + 1}$, the front Mach line from the opposite tip intersects the trailing edge at a value of $y_b = \frac{2(h - m)}{1 - m\beta}$ so that values for y_b in equation (B5) may be taken from $\frac{2(h - m)}{1 - m\beta}$ to $2h$ at the tip. (See fig. 2(b).)

(b) If the aspect ratio A is equal to or less than $\frac{2m}{m\beta + 1}$, the front Mach line from the opposite tip intersects the center section and values for y_b in equation (B5) may be taken from h to 2h. In this case, the increment in Δc_d discussed under type I is obtained at spanwise positions of y_a from -h to 0.

When $m = \frac{1}{\sqrt{M^2 - 1}}$, equation (B5) becomes:

$$\Delta c_{d_{II}} = \frac{8}{\pi}\left(\frac{t}{c}\right)^2 m \left\{ y_b'\left[\frac{1}{12}\left(7y_b' - 10h' - 2\right)\sqrt{y_b' - 2(h' - 1)^2 - y_b'^2} - \left(\frac{5}{4}y_b'^2 - 3h'y_b' + 2h'^2 - 1\right)\left(\cosh^{-1}\frac{y_b' - 2h' + 2}{y_b'}\right)\right] + \frac{2}{3}\frac{\left[2y_b'^3 - 6y_b'^2h' + 3y_b'\left(2h'^2 - 1\right) - 2h'^3 + 3h' - 1\right]\sqrt{1 - h'}}{\sqrt{y_b' + 1 - h'}} \right\}$$

The total increment in drag coefficient at a section caused by the tips is given by

$$\Delta c_d = \Delta c_{d_I} + \Delta c_{d_{II}}$$

and the total drag coefficient at the section is

$$c_d = c_{d_\infty} + \Delta c_d$$

Wing-Drag Coefficients

<u>Wing-drag coefficient without tip effects</u>.- If the aspect ratio is equal to or less than $\frac{2m}{1 - m\beta}$, the wing-drag coefficient without the tip effect is

$$C_{D_\infty} = \frac{8}{\pi}\left(\frac{t}{c}\right)^2 m \left\{\frac{A'^2}{12m'^3}\left(3A' \cosh^{-1}\frac{A' + 2m'}{A'm'}\right.\right.$$

$$\left. - 6A' \cosh^{-1}\frac{1}{m'} - \sqrt{A'^2\left(1 - m'^2\right) + 4m'(A' + m')}\right.$$

$$\left. + 2A'\sqrt{1 - m'^2}\right) + \frac{1}{3m'^3\sqrt{1 - m'^2}}\left[2m'^3 \cosh^{-1}\frac{A'\left(1 - m'^2\right) + 2m'}{2m'^2}\right.$$

$$+ \left(2m'^3 + 3A'm'^2 - A'^3\right) \cosh^{-1}\frac{A'\left(1 + m'^2\right) + 2m'}{2m'(A' + m')}$$

$$\left.\left. + \left(2A'^3 - 6A'm'^2\right) \cosh^{-1}\frac{1 + m'^2}{2m'}\right]\right\}$$

where $A' = A\beta$ and $m' = m\beta$

If the aspect ratio is greater than $\dfrac{2m}{1 - m\beta}$, the wing-drag coefficient without tip effect is,

$$C_{D_\infty} = \frac{8}{\pi}\left(\frac{t}{c}\right)^2 m\left(\frac{A'^2}{12m'^3}\left[3A'\left(\cosh^{-1}\frac{A' + 2m'}{A'm'} + \cosh^{-1}\frac{A' - 2m'}{A'm'}\right)\right.\right.$$

$$- 6A'\cosh^{-1}\frac{1}{m'} - \sqrt{A'^2\left(1 - m'^2\right) + 4m'(A' + m')}$$

$$\left. - \sqrt{A'^2\left(1 - m'^2\right) + 4m'(m' - A')} + 2A'\sqrt{1 - m'^2}\right]$$

$$+ \frac{1}{3m'^3\sqrt{1 - m'^2}}\left\{2m'^3\left[\cosh^{-1}\frac{A'\left(1 - m'^2\right) + 2m'}{2m'^2}\right.\right.$$

$$\left. - \cosh^{-1}\frac{A'\left(1 - m'^2\right) - 2m'}{2m'^2}\right]$$

$$+ \left(3A'm'^2 - 2m'^3 - A'^3\right)\cosh^{-1}\frac{A'\left(1 + m'^2\right) - 2m'}{2m'(A' - m')}$$

$$+ \left(3A'm'^2 + 2m'^3 - A'^3\right)\cosh^{-1}\frac{A'\left(1 + m'^2\right) + 2m'}{2m'(A' + m')}$$

$$\left.\left. + \left(2A'^3 - 6A'm'^2\right)\cosh^{-1}\frac{1 + m'^2}{2m'}\right]\right\}\Bigg)$$

Increment in wing-drag coefficient caused by wing tips.- If the aspect ratio of the wing is equal to or greater than $1/\beta$, the contribution of the wing tips to the wing-drag coefficient is zero.

If the aspect ratio of the wing is equal to or greater than $\frac{2m}{m\beta + 1}$, the total increment in C_D caused by the local tip, or ΔC_{D_I}, is zero; and the increment ΔC_D is obtained solely from the effect of the tip located on the opposite half of the wing, or $\Delta C_{D_{II}}$. For this case, integration of equation (B5) over the wing yields:

$$\Delta C_D = \frac{8}{\pi}\left(\frac{t}{c}\right)^2 m \left\{\frac{1}{3m'^3\sqrt{1 - m'^2}}\left[(A' - 2m')(A' + m')^2 \cosh^{-1}\frac{m'A' + 1}{A' + m'}\right.\right.$$
$$\left. + (A' + 2m')(A' - m')^2 \cosh^{-1}\frac{1 - m'A'}{|A' - m'|}\right]$$
$$\left. + \frac{A'}{3m'^3}\left[6m'^2 - A'^2\left(2 + m'^2\right)\right] \cosh^{-1}\frac{1}{A'} - \frac{A'}{3m'}\sqrt{1 - A'^2}\right\}$$

If the aspect ratio of the wing is less than $\frac{2m}{m\beta + 1}$, the increment ΔC_D is affected by both wing tips. For this case, integration of equations (B3) and (B5) yields:

$$\Delta C_D = \frac{8}{\pi}\left(\frac{t}{c}\right)^2 m\left(\frac{1}{3m'^3\sqrt{1 - m'^2}}\left[(A' - 2m')(A' + m')^2 \cosh^{-1}\frac{m'A' + 1}{A' + m'}\right.\right.$$
$$+ (A' + 2m')(A' - m')^2 \cosh^{-1}\frac{1 - m'A'}{|A' - m'|} - 2m'^3 \cosh^{-1}\frac{2m' - A'\left(1 - m'^2\right)}{2m'^2}$$
$$\left. - \left(2m'^3 - 3m'^2A' + A'^3\right) \cosh^{-1}\frac{2m' - A'\left(1 + m'^2\right)}{|2m'(m' - A')|}\right]$$
$$+ \frac{A'}{3m^3}\left\{\left[6m'^2 - A'^2\left(2 + m'^2\right)\right] \cosh^{-1}\frac{1}{A'} + \frac{A'}{4}\sqrt{4m'(m' - A') + A'^2\left(1 - m'^2\right)}\right\}$$
$$\left. + \frac{A'^3}{4m'^3} \cosh^{-1}\frac{2m' - A'}{m'A'} - \frac{A'}{3m'}\sqrt{1 - A'^2}\right)$$

Total wing-drag coefficient.- The total wing drag is obtained as the sum,

$$C_D = C_{D_\infty} + \Delta C_D$$

where the components C_{D_∞} and ΔC_D are calculated from the foregoing equations for the wing-drag coefficient appropriate to the aspect ratio of the wing.

Wing-drag coefficient for special case $m = \frac{1}{\beta}$.- When the Mach line coincides with the wing leading edge $\left(m = \frac{1}{\beta}\right)$, the wing-drag coefficient obtained for all aspect ratios as a limiting case $(m' \longrightarrow 1)$ is equal to the real part of the following expression:

$$C_D = \frac{8}{\pi}\left(\frac{t}{c}\right)^2 m \left(\frac{A'^3}{4}\left(\cosh^{-1}\frac{A'+2}{A'} + \cosh^{-1}\frac{2-A'}{A'}\right) + A'\left(2-A'^2\right)\cosh^{-1}\frac{1}{A'}\right.$$

$$\left. + \frac{1}{6}\left\{\left[3A'^2 + 2A'\left(1 - 3\sqrt{A'+1}\right) - 8\right]\sqrt{1-A'} + \left(8 + 2A' - 3A'^2\right)\sqrt{A'+1}\right\}\right)$$

Wing-Drag Coefficients at Mach Number of 1.0

The drag coefficient for the wing at $M = 1.0$ may be expressed in terms of the following formulas which were obtained by integrating over the wing the limiting values for c_d in equations (B1), (B3), and (B5) as the factor $\beta = \sqrt{M^2 - 1}$ approaches zero:

(1) If the aspect ratio of the wing is equal to or greater than $2m$

$$C_D = \frac{8}{3\pi}\left(\frac{t}{c}\right)^2 \frac{m}{h}\left(\int_0^2 m\left[\left(-K^3 + 6K + 4\right) \log_e (K + 2) - 3K^3 \log_e 2K\right.\right.$$

$$\left.+ \left(4K^3 - 6K - 2\right) \log_e (K + 1) + K^2(K - 2)\right] dK$$

$$+ \int_2^{h/m} m\left[\left(-K^3 + 6K - 4\right) \log_e (K - 2) - \left(K^3 - 6K - 4\right) \log_e (K + 2)\right.$$

$$\left.+ \left(4K^3 - 6K\right) \log_e \left(K^2 - 1\right) + 2 \log_e \frac{K - 1}{K + 1} - 6K^3 \log_e K\right] dK$$

$$+ \int_{h-2m}^{h} \left\{\left[\frac{(y - h)^3}{2m^3} + \frac{3(h - y)}{m} - 2\right] \left[\log_e 2(y - h + 2m)\right]\right.$$

$$+ \left[\frac{(y + h)^3}{2m^3} + \frac{3y\left(y^2 - h^2\right)}{m^3} - \frac{3(h + y)}{m}\right] \left[\log_e m(y + h)\right]$$

$$- \left(\frac{4y^3}{m^3} - \frac{6y}{m} - 2\right) \left[\log_e 2m(y + m)\right]$$

$$\left.\left.+ \frac{y + h}{4m^3}(7y - 3h - 2m)(y - h + 2m)\right\} dy\right) \tag{B6}$$

where $K = \frac{y}{m}$

In equation (B6), the first two integrals represent the drag coefficient for the wing without the tip effect; whereas, the last integral represents the effect of the tips $\Delta C_{D_{II}}$. For this case, in which the aspect ratio is equal to or greater than $2m$, the tip effect ΔC_{D_I} is zero; hence the integral for the section increments in c_d is not given in equation (B6). Equation (B6) has been solved for a sweepback angle of 45° and the results for this sweep angle may be converted to other wings of arbitrary sweepback by the formulas (13) to (15). For the wing of 45° sweepback, $m = 1$ and $A \geqq 2$, equation (B6) yields the following result:

$$C_D = \frac{2}{3\pi}\left(\frac{t}{c}\right)^2\left[\left(-A^3 + 12A + 16\right)\log_e (A + 2) + \left(-A^3 + 12A - 16\right)\log_e (A - 2) + 2A\left(A^2 - 12\right)\log_e A - 4A\right] \tag{B7}$$

(2) If the aspect ratio of the wing is smaller than $2m$, the upper limit of the first integral in equation (B6) is reduced from 2 to h/m, the second integral vanishes, and the lower limit for the third integral is reduced from $h - 2m$ to zero. For this case, however, in which the aspect ratio is less than $2m$, ΔC_{D_I} is not zero, and the following integral must be added to those in equation (B6) to obtain C_D:

$$\Delta C_{D_I} = \frac{8}{3\pi}\left(\frac{t}{c}\right)^2 \frac{m}{h}\int_{-h}^{0}\left[\left(\frac{{y_a}^3}{2m^3} - \frac{3y_a}{m}\right)\log_e \frac{2\left(y_a + 2m\right)}{my_a} + 2\log_e \frac{m^2}{y_a + 2m} + \frac{y_a\left(2m - 3y_a\right)\left(y_a + 2m\right)}{4m^3}\right] dy_a \tag{B8}$$

where

$$y_a = y - h$$

For the wing of 45° sweepback, $m = 1$, and $A < 2$, equations (B6) and (B8) yield the same result for C_D as that obtained for values of A greater than 2, as expressed by equation (B7). In this case, the real part of $\log_e(A - 2)$ is used.

REFERENCES

1. Jones, Robert T.: Thin Oblique Airfoils at Supersonic Speed. NACA TN No. 1107, 1946.

2. Puckett, Allen E.: Supersonic Wave Drag of Thin Airfoils. Jour. Aero. Sci., vol. 13, no. 9, Sept. 1946, pp. 475-484.

3. Göthert, B.: Ebene und räumliche Strömung bei hohen Unterschallgeschwindigkeiten (Erweiterung der Prandtlschen Regel). Bericht 127 der Lilienthal-Gesellschaft für Luftfahrtforschung, 1940, pp. 97-101.

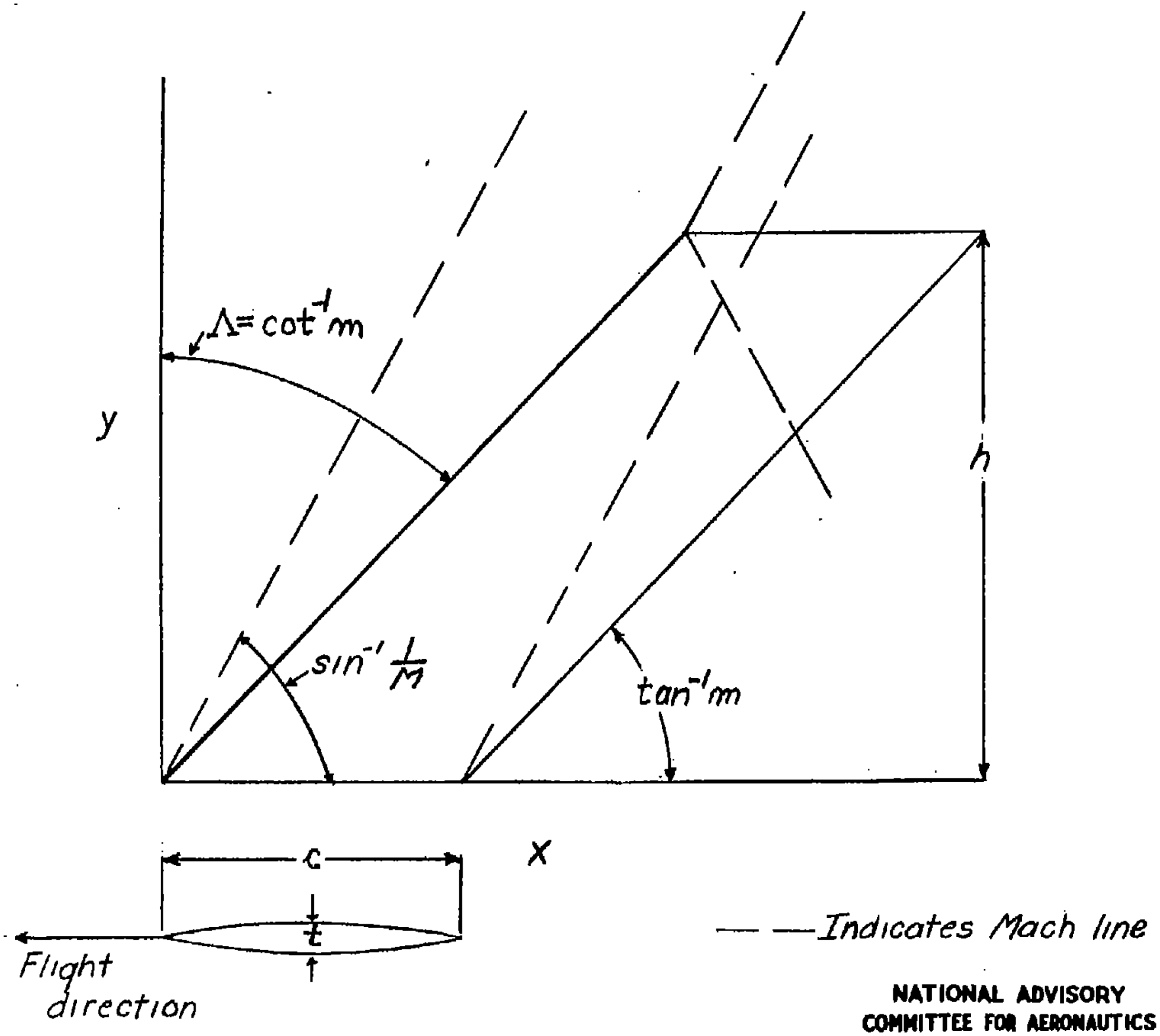

Figure 1.– Symbols for swept-back wing.

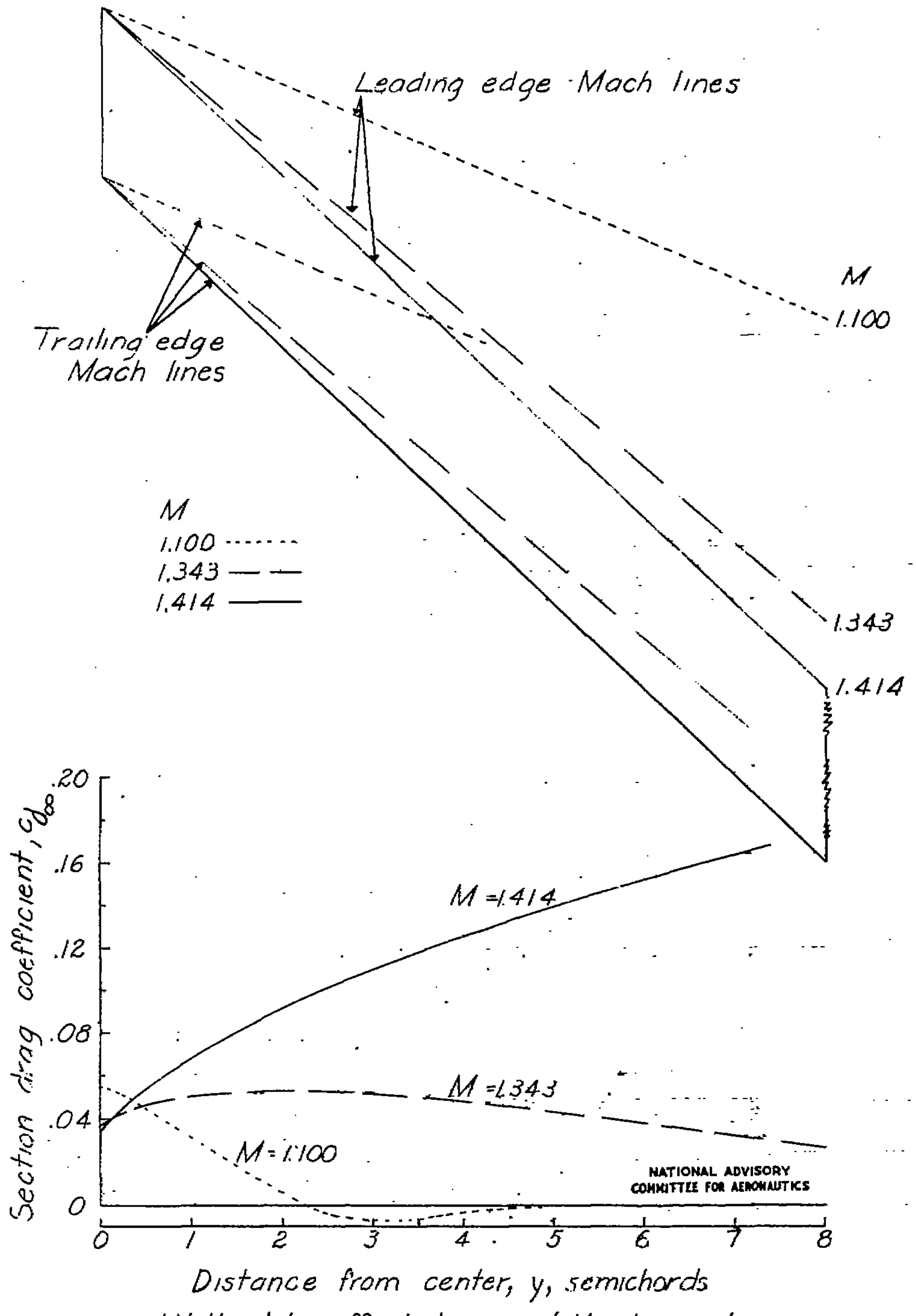

(a) Without tip effect at several Mach numbers.

Figure 2.— Typical distributions of section wave-drag coefficients along wing span. Biconvex profile at zero lift; sweepback angle, 45°; thickness ratio in flight direction, 0.10.

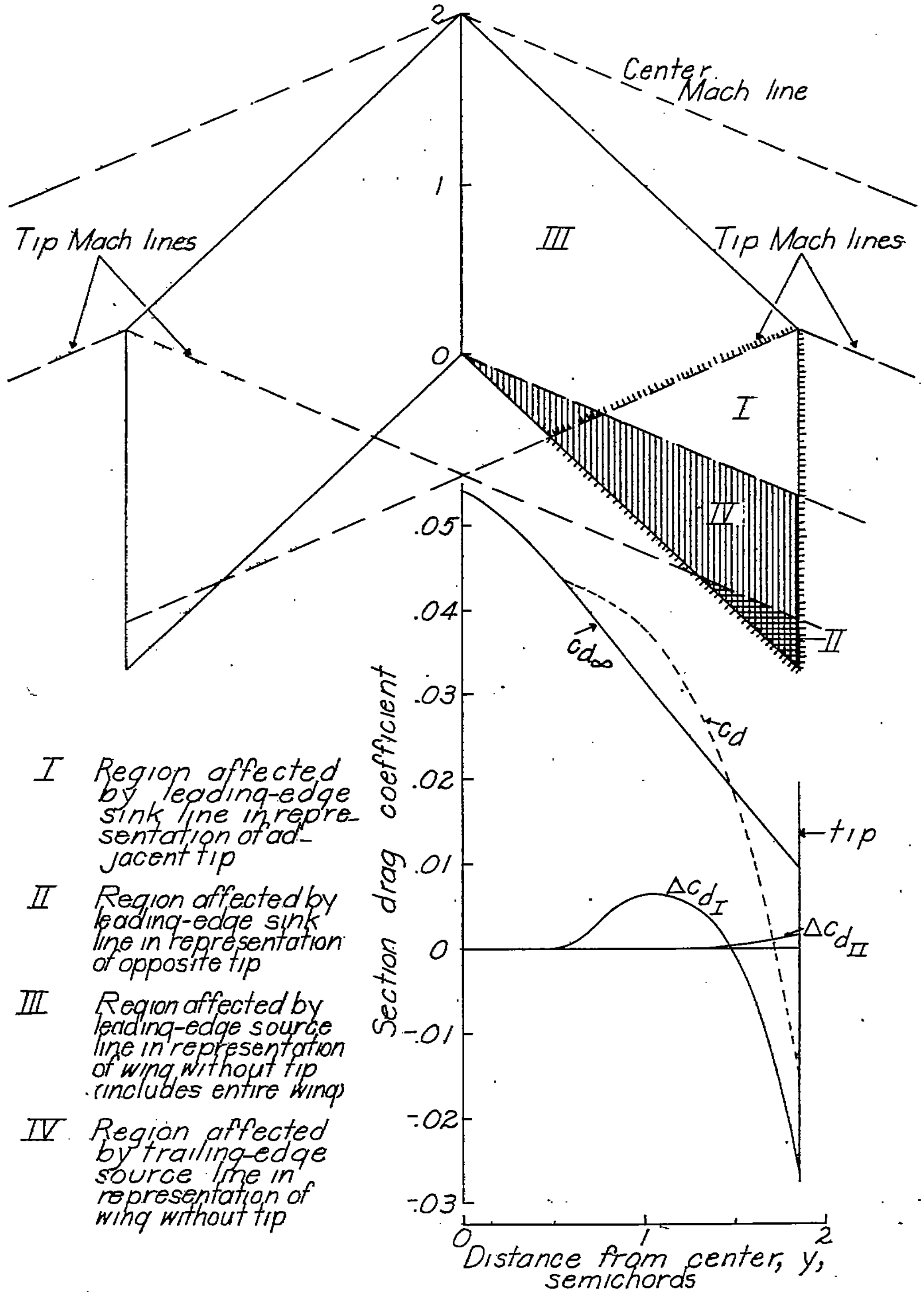

(b) With tip effect. Aspect ratio, 1.86; Mach number, 1.10.

Figure 2.—Concluded.

NATIONAL ADVISORY COMMITTEE FOR AERONAUTICS

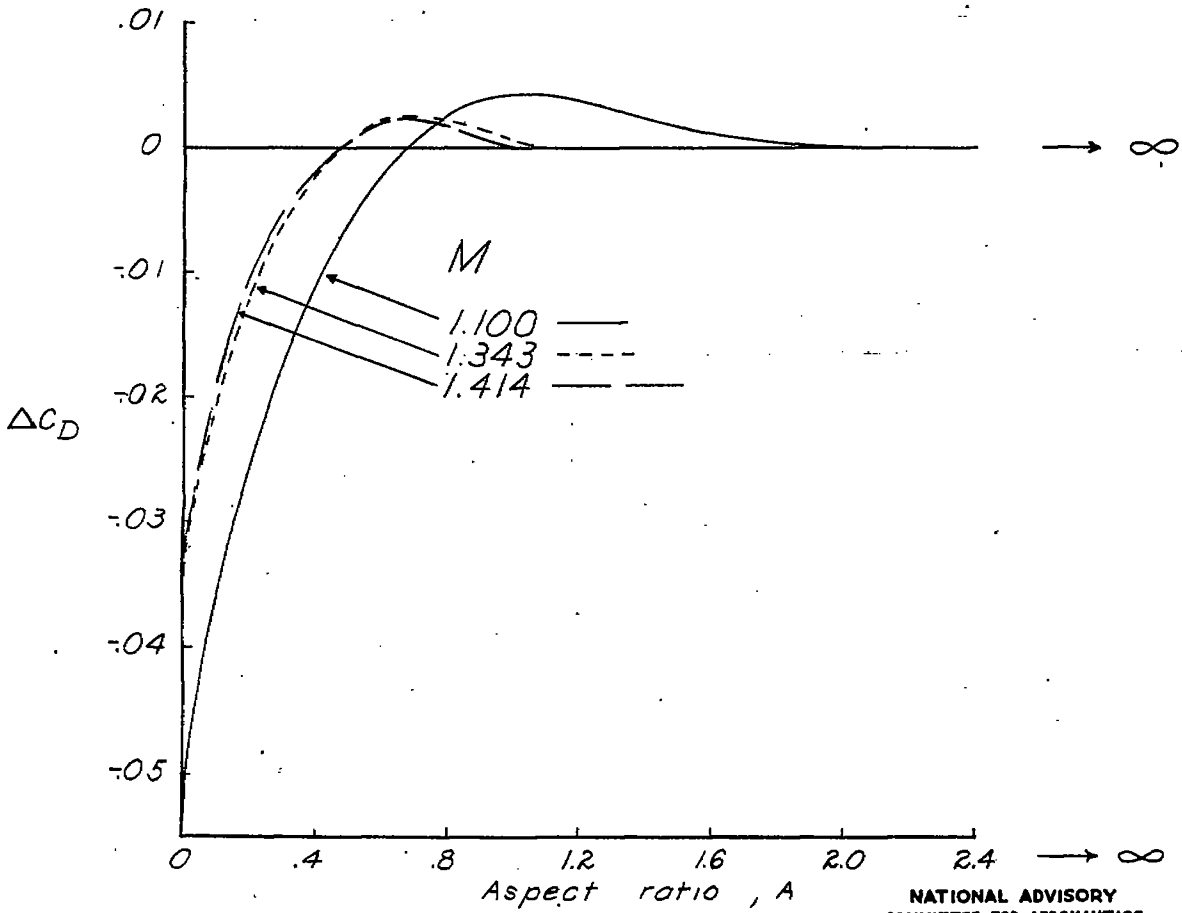

Figure 3.– Typical variations with aspect ratio of the increments in wing wave-drag coefficient caused by wing tips at different Mach numbers. Biconvex profile at zero lift; sweepback angle, 45°; thickness ratio in flight direction, 0.10.

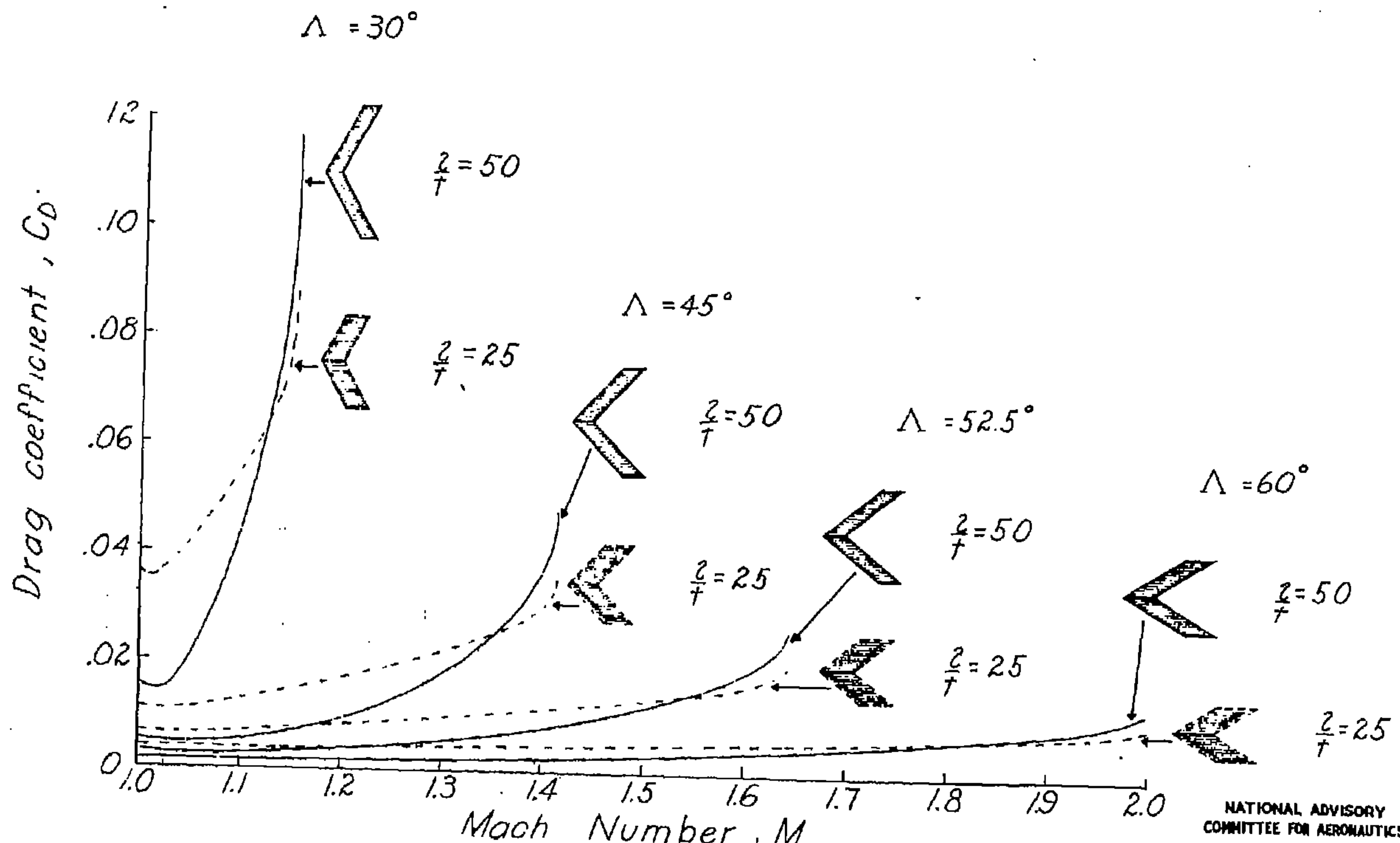

NATIONAL ADVISORY COMMITTEE FOR AERONAUTICS

Figure 4.– Variation with Mach number of wing wave-drag coefficient for different sweepback angles with constant slenderness ratios. Biconvex profile at zero lift; $A = 0.20\frac{l}{t}\cos^2\Lambda$; $\frac{t}{c} = 0.10\cos\Lambda$; constant wing area.

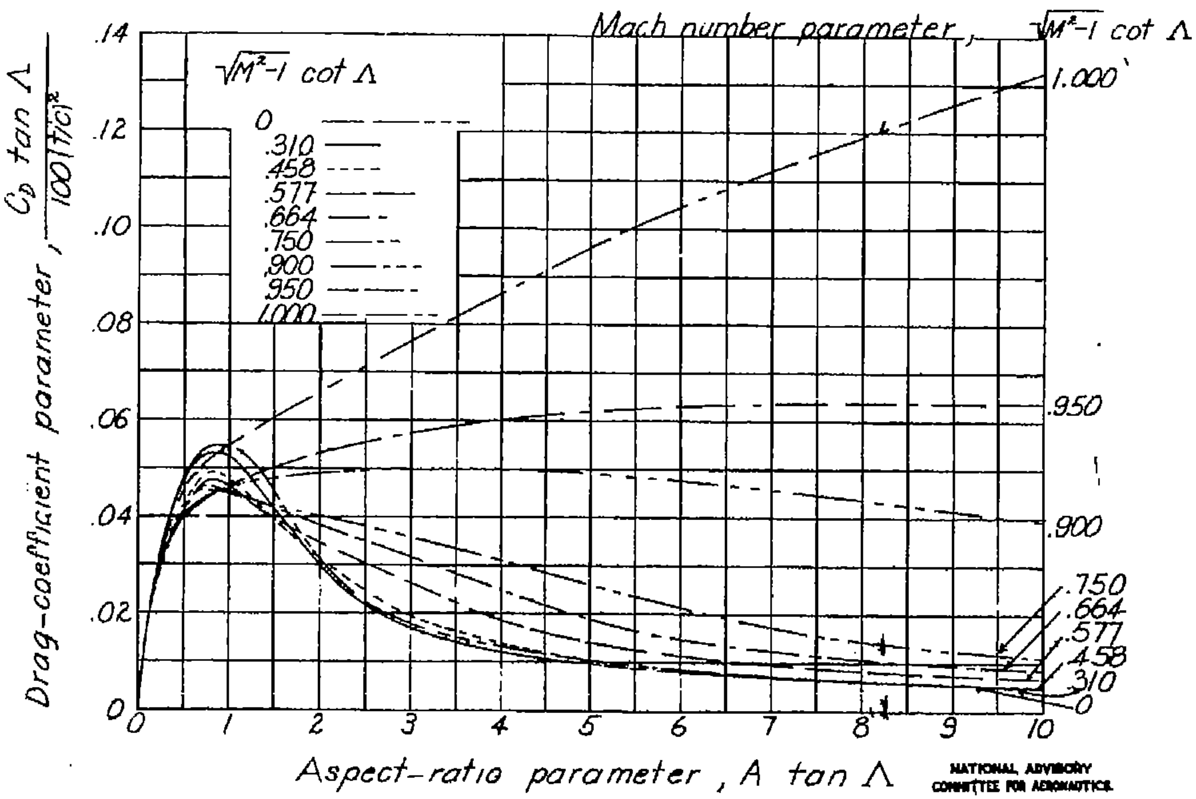

Figure 5.– Generalized curves for variation of wing wave-drag coefficient with aspect ratio for constant sweepback angles, Mach numbers, and thickness ratios. Biconvex profile at zero lift.